Periodica Polytechnica Chemical Engineering, 68(3), pp. 454–469, 2024

Experimental and Regression Vapor–liquid Equilibrium Data for Ethanol + Dipropylene Glycol Binary System

Ethanol Anhydrization Process Simulation Using Dipropylene Glycol as Extractive Agent

Marilena Nicolae[1*], Elena M. Fendu[1]

[1] Petroleum Processing Engineering and Environmental Protection Department, Petroleum-Gas University of Ploieşti, blvd. Bucureşti, 39 no., 100680 Ploieşti, Romania
[*] Corresponding author, e-mail: mnicolae@upg-ploiesti.ro

Received: 12 September 2023, Accepted: 31 January 2024, Published online: 06 June 2024

Abstract

Ethanol is one of the most utilized additives in gasoline, and its obtaining and separation from regenerable resources is of great interest. Despite the enormous energy consumption, extractive and azeotropic distillation is still preferred for ethanol anhydrization. This work studies the utilization of dipropylene glycol (DPG) as an extractive agent. The vapor–liquid equilibrium (VLE) data for the ethanol + DPG binary system was experimentally determined and the VLE data obtained were regressed using Non-Random Two Liquid (NRTL) and Universal Quasi Chemical (UNIQUAC) thermodynamic models in PRO/II 2020 simulation software. The binary interaction parameters obtained from regression were used to simulate the water + ethanol separation by extractive distillation with DPG. There were realized a series of several simulations, using different solvent/feed ratios in the extractive distillation column, starting from two basic variants: variant A, where no heat recovery is considered, and variant B, where the heat of the hot streams in the process flow diagram (PFD) is recovered in three heat exchangers. The specific energy consumption (SEC) expressed as MJ/kg of anhydrous ethanol were calculated for each variant. It was found that the most economical is variant B which for the SEC is 7.53 MJ/kg of anhydrous ethanol. The SEC calculated for the best variant in this study is lower than the SEC calculated by other researchers for similar processes.

Keywords

bioethanol, dipropylene glycol, VLE, anhydrization, extractive distillation

1 Introduction

The lack of fossil fuels is one of the major problems in modern society. Thus, regenerable energy and fuel resources are intensively investigated. Among the bio combustibles, bioethanol is the most promising short-term alternative, and it is already used as an additive in gasoline in various percentages in most of the world's countries. Moreover, bioethanol production can be easily integrated with biodiesel production.

On world wide's level, bioethanol is the most utilized biofuel for transportation. Bioethanol and the mixtures of bioethanol and gasoline have a long history as alternative fuels for transportation.

Bioethanol cannot be used singly as fuel, but only in modified engines. Nowadays, bioethanol is mixed with gasoline in the following proportions: 5 vol.% bioethanol + 95 vol.% gasoline (mixture known as E5 according to the EU standard EN 228 [1], 10 vol.% bioethanol + 90 vol.% gasoline (E10). The mixtures containing gasoline and bioethanol up to 25 vol.% (between 5 and 25%) are known as "gasohol". Many countries (USA, Canada, Sweden, Brazil [2] have exerted their biofuels plan in the form of mixtures of gasoline and biofuels in different proportions – mixtures known as FFV for vehicles with flexible engines.

To be used as fuel or as an additive, the bioethanol must have a purity of a minimum of 99 wt.% (between 99.0 and 99.8 wt.%, i.e. 97.48 mole% and 99.49 mole% ethanol) according to the international standard EN 15376 [3]. The largest amount of water from bioethanol is removed by distillation, but the purity of bioethanol is limited to 89.47 mole% ethanol because of the minimum azeotrope with the water. The industrial processes used at this moment for ethanol anhydrization are extractive distillation [4–13], azeotropic distillation [7, 14–18] adsorption [19–22], pervaporation [23, 24] or pressure swing distillation [25, 26]. Hybrid

Cite this article as: Nicolae, M., Fendu, E. M. "Experimental and Regression VLE Data for Ethanol + DPG Binary System: Ethanol Anhydrization Process Simulation Using DPG as Extractive Agent", Periodica Polytechnica Chemical Engineering, 68(3), pp. 454–469, 2024. https://doi.org/10.3311/PPch.23426

processes that combine membrane processes with distillation claim the smallest costs for the separation of bioethanol obtained from fermented broths. For example, micro bubble distillation separates the components at temperatures lower than the boiling point of the azeotrope. It has the advantage of lower energy requirement, but the process includes the study of the complex microbubble dynamics, a study still under development [19]. The pervaporation distillation hybrid process offers flexibility concerning load and feed conditions and has the advantage of no contamination of the products but has the disadvantage of the concentration polarization on the feed side and the temperature reduction along the module [19].The adsorption-desorption process for ethanol anhydrization presents one of the most straightforward types of equipment in the literature, with sufficient data, but requires continuous regeneration of the adsorbent. Regeneration of the adsorbent implies energy consumption in the desorption step. Moreover, often is encountered the fouling of the adsorbent by cells. Processes based on membrane dephlegmator consist of a combination of distillation and pervaporation in a single unit. The process has a small footprint, being thermodynamically efficient and ensuring the elimination of the azeotrope. Still, due to its complexity, it isn't easy to operate the process at an industrial scale. Furthermore, the process does not have a significant recovery degree [19]. The literature offers a large amount of information regarding the specific energy consumption (SEC) expressed as MJ/kg bioethanol or as a price for a liter of ethanol ($ or €/liter of bioethanol produced) for the hybrid processes. The studies published now show different purification schemes, starting from different concentrations of the aqueous solution of ethanol (4.16 mole%, 36.97 mole%, 61 mole% or 68.9 mole% ethanol). For example, Wang Y. and co-authors [20] reported a SEC of 1.3 MJ/kg ethanol for purification of a concentrated solution (64.05–82.83 mole% ethanol in water) using starch-based adsorbents; Singh A. and co-authors [25] have found that for a process of distillation assisted by a heat pump combined with pressure swing adsorption (PSA), the SEC is 3.2 MJ/kg ethanol, 38% less than in the case of conventional distillation. Other researchers have stated that the SEC is insufficient to reflect the actual cost of ethanol production, so they calculated the cost of manufacture (COM), which includes the capital and operational costs. This way, Hanchate and co-authors [22] reported in 2019 a total price of 1 130 947.18 US$ for a production of 6 094 ton/year, which means 185.8 US$/ton of anhydrous ethanol for a hybrid process of Temperature Swing Adsorption (TSA) while Loy [26] has found that for a Pressure Swing Adsorption (PSA) process with a production of 200 000 m^3/year (starting from a diluted solution of 4.16 mole% ethanol), the COM is 19 126 000 US$/year, that meaning 118.5 US$/ton of anhydrous ethanol. Roth and co-authors [21] have found that for a combined process (distillation and adsorption) for purification of the ethanol solutions, the SEC is situated between 83.92 €/ton and 106.96 €/ton of anhydrous ethanol, depending on the concentration of the solution (81.81 mole%, 61 mole%, 24.24 mole% ethanol in water).

The study achieved by Botshekan and co-authors [27] presents economically viable strategies in nine proposed scenarios for further energy reductions in a commercial case study for ethanol production. The base case consists of a conventional three-column separation system without column heat integration. The authors proposed reducing the high operating costs of bioethanol production plants by employing thermally coupled columns, dividing-wall column and heat integration, and multistage pervaporation. The multi-stage pervaporation module handled the azeotropic mixture among different bioethanol dehydration methods and resulted in the highest fossil energy ratio and profitability index. The optimized four-stage pervaporation module seems to be an efficient alternative method to pressure swing adsorption for bioethanol dewatering.

Extractive distillation is a process widely used for ethanol anhydrization. In the literature, many compounds or mixtures are mentioned to be used as solvents (dissolvents). The most studied and reported solvent is ethylene glycol (EG) [4–8]. Still, there are studies on other compounds such as: glycerol [9], solutions of salts such as NaCl, KCl, $CaCl_2$, Na-acetate, K-acetate [10], octanol, iso-octanol, and mixtures of these with octanoic acid [5], deep eutectic solvents (DES) or low-temperature transition mixtures (LTTMs), as choline chloride/urea (ChCl/urea 2:1) [11, 12] and glycolic acid/choline chloride (glycolic acid/choline chloride 3:1) [13].

The processes for ethanol purification based on azeotropic distillation are energy-intensive due to large consumption in the reboilers of the distillation columns. Depending on the boiling temperature of the entrainer, the energy consumption varies. Different compounds were proposed as entrainers for azeotropic distillation: methyl *tert*-butyl ether (MTBE) [14, 15], ethyl *tert*-butyl ether (ETBE), *tert*-amyl methyl ether (TAME), diisopropyl ether (DIPE) [14, 16] isooctane [15, 17], octane, [18], hexane, cyclohexane, gasoline [16], [17], pentane [7]. The SEC for these processes varies between 1.69 MJ/kg ethanol [17] and 8 MJ/kg ethanol [15], depending on the ethanol concentration in the feed.

The major problem of azeotropic and extractive distillation methods is the significant energy demand, which leads to high operation costs. The new proposed alternatives

must decrease these costs, taking into account the high demand for bioethanol. The researchers have proposed alternatives to conventional extractive and azeotropic distillation, such as extractive and azeotropic distillation in dividing wall columns [6, 7, 28].

This study is among those research studies to find a method for separating the water + ethanol mixture using extractive distillation. Dipropylene glycol (DPG) was not mentioned in the literature until now as an extractive agent for ethanol + water separation. As mentioned in the Safety data sheet [29], DPG is used as solvent in the industrial applications, is not a hazardous substance, is biodegradable in a proportion of 84.4%, the only recommended safety measure when handling the substance being the wearing of the protective glasses. Also, it is mentioned that DPG is not harmful for human, but for the bacteria, aquatic invertebrates, for fishes and other aquatic plants and algae. Nevertheless, it was used as solvent for aromatics extraction from gasoline [30, 31]. In this work, DPG is studied as a possible extractive agent for the extractive distillation process applied for ethanol + water separation. Considering that dipropylene glycol wasn't mentioned in the literature as an extractive agent for ethanol, but just the propylene glycol [32], it was found that there are no equilibrium data published until now between ethanol and dipropylene glycol, but only for water and dipropylene glycol [31, 33]. We determined the vapor-liquid equilibrium (VLE) data for the binary system ethanol + dipropylene glycol, and the data are presented in this work. The VLE data are mandatory in the simulation of a new proposed process for the correctness of the process design.

2 Experimental determination and regression of the VLE data for ethanol + DPG

2.1 Materials

The chemicals used in this study are ethanol and dipropylene glycol; they were supplied by Sigma-Aldrich and Dow-Chemical. Dow Chemical is one of the main suppliers for propylene glycols, and additional information about toxicity and safety can be found in the safety data sheet available on the supplier's website. Detailed information on the chemicals used in the experimental part of this work, such as abstracts registry number (CAS number), the stated purity by the suppliers, and sources, are given in Table 1. All liquids were used without further purification. Water content was determined with the Cou-Lou Karl Aquamax apparatus through the volumetric Karl Fischer volumetric titration analysis method (with accuracy value of ±0.5%). It was determined that DPG has an 0.003 weight % water, while ethanol is almost pure; the supplier (Sigma Aldrich) reported a purity of ≤ 100 % ethanol. The standard procedure for VLE data determination requires degassing each sample before reaching the equilibrium state. Pure liquids and each mixture were cooled using a cooling bath, by bringing them near to the freezing point and then were degassed by achieving a pressure very close to 0 absolute of pressure just before the experiment using a vacuum pump. The pressure was measured using a DPI 705 sensor with a measuring range of up to 100 kPa. The temperature was measured with VWR International, LLC, NIST traceable digital thermometer (± 0.05 % accuracy and 0.001 K resolution).

Table 1 Specifications of the chemicals used in experimental determinations.

Chemical Name	CAS #	Molar mass (g/mol)	Molar fraction purity (as stated by the supplier)	Supplier
Ethanol	64–17–5	46.07	0.9949	Sigma-Aldrich
Dipropylene glycol	25265–71–8	134.2	0.9919	Dow-Chemical

2.2 Apparatus and procedure

The vapor-liquid equilibrium experimental data of the ethanol + DPG binary system were realized using a static equilibrium apparatus built in our laboratory, schematically presented in Fig. 1. This static apparatus has a range of

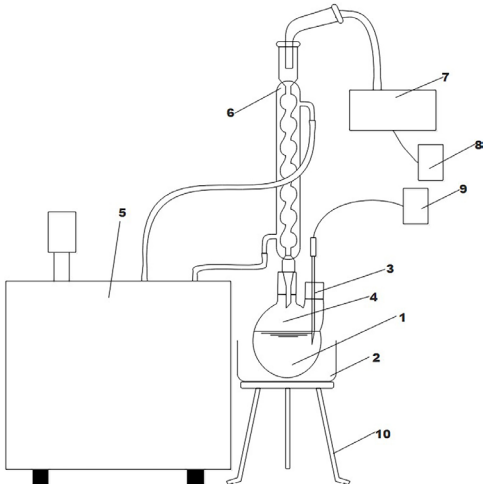

Fig. 1 Operation scheme of the static apparatus used to determine vapor-liquid equilibrium experimental data. 1, the sample of the mixture to be analyzed; 2, heating mantle; 3, temperature sensor; 4, equilibrium cell 5, constant temperature bath (cold reservoir source); 6, ascending condenser; 7, vacuum equipment; 8, digital pressure indicator; 9, digital thermometer; 10 support.

advantages: the data are determined quite rapidly, the procedure is simple and does not implies very expensive methods for sample analysis. Moreover, before the experimental determinations, we made a series of theoretical analysis of the binary ethanol + DPG, i.e., we determined the *T-x-y* diagram with the UNIFAC predictive model [34] and then with IDEAL [35] model using PRO/II simulation software, and we observed that the *T-x-y* diagram calculated with UNIFAC does not have an irregular shape, specific to non-ideal systems. The diagrams calculated with UNIFAC and IDEAL thermodynamic models have the same shape. Taking all these into account, we decided to use the static apparatus for the VLE determination of the binary system ethanol + DPG.

Samples of ethanol + DPG mixture were previously prepared. The composition of the samples was calculated in molar fractions, using exact quantities of pure components, weighted with an analytical balance (Mettler Toledo AB204-S electronic balance with an accuracy of 0.0001 g).

A sample of the ethanol + DPG mixture with a known composition is introduced into the equilibrium cell (4). The cell is connected to an ascending condenser (6) that cools the ethanol vapor using the condensing agent from a constant temperature bath (5) which passes through the condenser's mantle. After degassing, the pressure will be set to the value of the pressure at which it is desired to determine the boiling point temperature. The pressure is formed using vacuum Eq. 7. The cell is heated with a heating mantle (2). By heating, the sample generates vapors that are condensed in the ascending condenser and returned to the initial liquid phase in the cell. When the temperature remains constant (the value of the temperature doesn't change for 30 minutes), the pressure in the system is measured using a pressure sensor and a digital pressure indicator (8), while the temperature is measured using a temperature sensor (3), and digital thermometer (9).

During the experiment more than 90% of the close equilibrium cell volume is occupied by the liquid phase, thus at the equilibrium the vapors quantity is very small and does not affect the liquid phase.

Regarding the liquid composition at the equilibrium, there is assumed it is no change, as long, the small quantity of vapors are condensed and returned into the equilibrium cell, using a cooling agent with a low temperature. Thus the sample remains every time in the closed equilibrium cell. At each pressure, maintained constant for a sufficiently long time to achieve the equilibrium, the temperature is measured. Three replicates were performed for each experimental determination.

The validation of the procedure for the VLE determination and the data obtained with this apparatus was achieved earlier by the determination of the VLE data for the water + DPG binary system. For the binary system water + DPG, the VLE data were obtained by a static apparatus described by Fendu and Oprea [33]. The data obtained with the static apparatus illustrated in Fig. 1 were compared with those obtained with the apparatus described in [33] for the water + DPG binary. They were in good agreement, as can be observed in Fig. 2. The authors have chosen to present the data for validation of the method as a figure and not as a table and not to replicate the data because it is desired to make a visual comparison between the data determined with the two mentioned methods. In Fig. 2 there are represented the boiling point data (depicted by the full circle) determined to validate the technique applied in this work to determine the pressure-temperature-mole fraction (*P-T-x*) data for the ethanol + DPG binary system. The experimental VLE data for the binary system water + DPG determined by Fendu and Oprea with the static apparatus described in their work [33] are depicted with a continuous line, and as we can see, they are in good agreement with the data determined as boiling points at constant pressures, there being small deviation just for the smallest concentration of water in solution (for the data determined with the solution of 0.3005 mole fraction of water).

Also, another well known method for the validation and checking of the consistency of VLE data is the "Arc test". This method, described by Van der Linde and coauthors [36] was applied to check the consistency of the VLE data determined in this work for the pure components. Oonk and Van der Linde [37] observed that "for data assessment the optically straight line has the disadvantage that

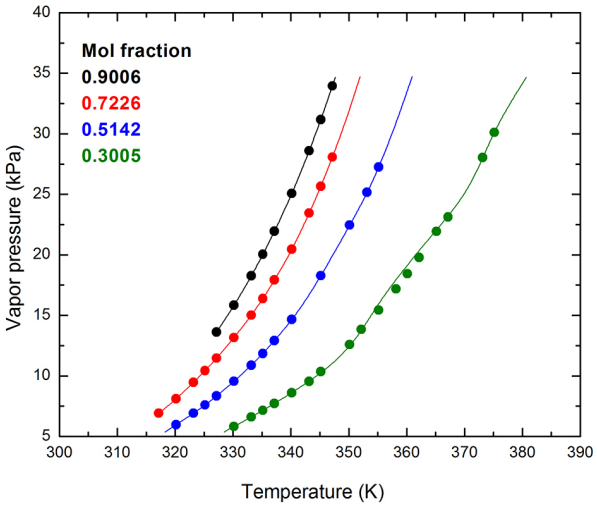

Fig. 2 Comparative *P-T-x* data for the binary system water + DPG: full circle – data determined with apparatus described in this work; continuous line – data determined by Fendu and Oprea [30].

subtle features of the experimental data set remain hidden". To repair this disadvantage, they proposed a graphical method in which the physical significance of the data is conserved by the addition of a linear contribution in $1/T$ by which the sensitivity of the ordinate axis is amplified by replacing $\ln(p/p_0)$ with $\ln(f)$. The expression of the equation applied for the arc test is given by the Eq. (1):

$$\mathrm{In}\left(f\right) = \mathrm{In}\left(p/p_0\right) - \alpha + \beta/T\,, \tag{1}$$

where, p is vapor pressure determined experimentally; p_0 = 1 Pa; T is the experimental temperature, expressed in K; the constants α and β are selected such that ln (f) is equal or close to zero for the two extreme pairs of a data set. For a good data set, the resulting figure has the appearance of an arc.

The arc test was applied for the pure components implied in this work ($x = 1$, ethanol and $x = 0$, DPG) using the data presented in Table 2, and the results are shown in Fig. 3 (a), (b).

2.3 Measurements results and data regression.

Table 2 presents the VLE measurements for the binary mixture ethanol + DPG in the 307.46 K to 502.56 K temperature range and pressure range of 13.332 kPa to 93.435 kPa. In Table 2, x refers to the concentration of ethanol in the liquid phase, expressed in mole fraction. Also, $u(T)$, $u(p)$, and $u(x)$ refer to the standard uncertainty of the temperature, pressure, and concentration of ethanol in the liquid phase.

The consistency of the *P-T-x* data was determined by two methods, namely: the arc test, as described above, using Eq. (1), and a procedure described by NIST [38, 39] that normally it is applied for pure components, but it can be extended also for mixtures. As the arc test, the consistency between the "end-points" of the VLE curve is checked. Next notations as adopted:

$$p_{\mathrm{bubble}}\left(x_1 \to 1\right) = p_1^0 \text{ and } p_{\mathrm{bubble}}\left(x_1 \to 0\right) = p_2^0\,. \tag{2}$$

The quality factor associated with the Pure Component Consistency Test is defined as:

$$F_{\mathrm{pure}} = \frac{2}{100\left(\Delta p_1^0 + \Delta p_2^0\right)}, \tag{3}$$

with limits $1 \le \Delta p_1^0,\ \Delta p_2^0 \le 10$

$$\text{and } \Delta p_1^0 = \left|\frac{p_{\mathrm{bubble}}\left(x_1 \to 1\right) - p_1^0}{p_1^0}\right|, \tag{4}$$

$$\Delta p_2^0 = \left|\frac{p_{\mathrm{bubble}}\left(x_1 \to 0\right) - p_2^0}{p_2^0}\right|. \tag{5}$$

For the consistent data, values of Δp_1^0 and Δp_2^0 have lower limits of 1. If the vapor pressure agrees within 1% of p_0 for both components, the factor F_{pure} is 1. If the vapor-pressure inconsistency is larger, the factor is smaller with a lower limit of 0.1 according to NIST.

The graphs corresponding to the arc test for all the mixtures presented in Table S2 and in Figs. S1–S5 can be found in the Supplement. Also, the values of α and β constants for all the mixtures can be found in Table S1 of the Supplement.

The values of Δp_1^0 and Δp_2^0 corresponding to the NIST consistency test are presented in Table S2 that can be also found in the Supplement. The values Δp_1^0 of and Δp_2^0 are below 0.01, so F_{pure} factor is considered 1 for the considered experimental set.

Knowing the actual vapor liquid balance is crucial for correctly designing an industrial distillation process and the raw VLE data cannot be used in the simulation of the processes, they must be processed to be used for a wider interspace of operation parameters. Thus, the raw *P-T-x* data were regressed to obtain the binary interaction parameters of the Non Random Two Liquids (NRTL) and Universal Quasi Chemical (UNIQUAC) thermodynamic system, specific to the binary systems (ethanol + DPG and water + DPG) involved in the process. The NRTL model (with three, five, and eight parameters named NRTL3, NRTL5, and NRTL8 subsequently) [40] and the UNIQUAC model (with two and four parameters, named UNIQUAC2 and UNIQUAC4 subsequently) [41] were used to correlate the experimental results. These thermodynamic models are based on the concept of local concentration, and thus, they give better results than other models.

The experimental data are regressed using the PRO/II [42] simulation software with default objective function (Eq. 6). The objective function (S) represents the minimization of the sum of squares for the relative deviations of calculated vapor pressure (P_{icalc}) from experimental vapor pressure (P_{iexpt}).

$$S = \sum_{i=1}^{N}\left(1 - \frac{P_{icalc}}{P_{iexpt}}\right)^2. \tag{6}$$

The NRTL parameters are succinctly presented in Eqs. 7–11 and the UNIQUAC parameters in Eqs. 12–19, as available in the PRO II reference manual [42]. The parameters of these equations were obtained by minimizing the objective function. Further there are displayed the main equations of NRTL model.

$$ln\gamma_i = \frac{\sum_j \tau_{ji} G_{ji} x_{ji}}{\sum_k G_{ki} x_k} + \sum_j \frac{x_j G_{ij}}{\sum_k G_{kj} x_k}\left(\tau_{ij} - \frac{\sum_k x_k \tau_{kj} G_{kj}}{\sum_k G_{kj} x_k}\right), \tag{7}$$

$$\tau_{ji} = a_{ij} + \frac{b_{ij}}{T} + \frac{c_{ij}}{T^2},\ \text{when unit is K}\,, \tag{8}$$

Table 2 Experimental VLE data for pressure p, temperature T with standard uncertainty $u(T)$, and mole fraction x for the system ethanol (1) + dipropylene glycol (2)*

p/kPa	T/K	$u(T)$/K	p/kPa	T/K	$u(T)$/K
		x=0.0000			
13.332	442.87	0.01	46.663	479.63	0.03
19.998	454.15	0.01	53.329	483.90	0.03
26.664	462.5	0.03	66.661	491.19	0.03
33.331	469.19	0.02	79.993	497.29	0.04
39.997	474.79	0.02	93.325	502.56	0.04
		x=0.1003			
13.352	363.15	0.02	47.044	410.03	0.03
20.530	376.06	0.02	53.271	415.41	0.05
26.763	388.11	0.02	66.716	424.81	0.05
33.337	396.20	0.02	80.063	432.25	0.04
40.098	404.15	0.03	93.325	438.70	0.06
		x=0.2003			
13.391	340.15	0.02	46.672	381.84	0.03
20.041	354.49	0.02	53.349	385.98	0.04
26.664	363.39	0.02	66.709	394.44	0.05
33.408	370.61	0.03	79.985	400.26	0.05
40.053	376.70	0.03	93.345	405.71	0.06
		x=0.3006			
13.352	331.23	0.02	46.665	367.79	0.03
20.056	346.71	0.02	53.546	371.88	0.05
26.724	355.25	0.02	66.792	378.95	0.06
33.433	359.59	0.03	79.972	385.24	0.05
40.145	363.98	0.04	93.332	390.25	0.07
		x=0.4015			
13.403	325.40	0.01	46.672	358.18	0.03
20.093	336.63	0.02	53.438	362.05	0.03
26.718	343.75	0.02	66.773	368.45	0.03
33.389	350.15	0.03	79.933	373.85	0.03
40.071	354.15	0.03	93.320	379.40	0.04
		x=0.4990			
13.423	321.35	0.02	46.723	352.12	0.03
20.080	331.45	0.02	53.431	355.08	0.03
26.808	338.68	0.02	66.709	361.26	0.04
33.460	345.05	0.03	79.967	366.32	0.04
40.105	348.73	0.03	93.435	370.69	0.05
		x=0.6000			
13.470	318.74	0.02	46.769	348.64	0.03
19.998	329.65	0.02	53.439	350.83	0.03
26.791	334.23	0.02	66.672	355.86	0.04
33.345	340.28	0.03	80.032	362.05	0.04
40.081	345.15	0.03	93.364	364.42	0.05

Table 2 Experimental VLE data for pressure p, temperature T with standard uncertainty $u(T)$, and mole fraction x for the system ethanol (1) + dipropylene glycol (2)* (continued)

p/kPa	T/K	$u(T)$/K	p/kPa	T/K	$u(T)$/K
		x=0.7004			
13.495	316.95	0.02	46.769	342.97	0.04
20.056	325.70	0.01	53.409	346.25	0.03
26.700	331.30	0.02	66.688	351.30	0.03
33.336	336.40	0.02	79.976	355.77	0.04
39.997	339.80	0.03	93.392	360.08	0.05
		x=0.8004			
20.114	321.57	0.02	53.446	342.85	0.04
26.668	327.68	0.02	66.658	348.22	0.03
33.313	331.98	0.02	79.968	352.71	0.03
40.113	336.22	0.02	93.361	356.60	0.04
46.673	339.70	0.03			
		x=0.8990			
20.154	317.67	0.02	53.421	339.82	0.03
26.546	323.98	0.02	66.665	344.88	0.04
33.380	328.90	0.02	80.020	349.41	0.05
40.061	332.92	0.03	93.335	353.20	0.04
46.732	336.59	0.03			
		x=1.000			
13.332	307.46	0.01	46.663	332.97	0.02
19.998	315.2	0.01	53.329	335.99	0.02
26.664	320.98	0.01	66.661	341.18	0.03
33.331	325.64	0.02	79.993	345.57	0.03
39.997	329.57	0.02	93.325	349.38	0.04

* Standard uncertainties u are $u(p)$ = 0.16 kPa and $u(x)$ = 0.0020.

$$\tau_{ji} = a_{ij} + \frac{b_{ij}}{RT} + \frac{c_{ij}}{R^2T^2}, \text{ when unit is kcal or kJ}, \quad (9)$$

$$G_{ij} = \exp\left(-\alpha_{ji}\tau_{ij}\right), \quad (10)$$

$$\alpha_{ji} = \alpha'_{ji} + \beta'_{ji}T\ . \quad (11)$$

Where:

- a, b, c – binary interaction parameters of the NRTL model;
- G – adjustable parameter which depends on the interaction energy between molecules of component "i" and component "j";
- R – universal gas constant J/(mol K);
- T – temperature (K);
- x – concentration of the component in the liquid phase of the mixture expressed as a mole fraction;

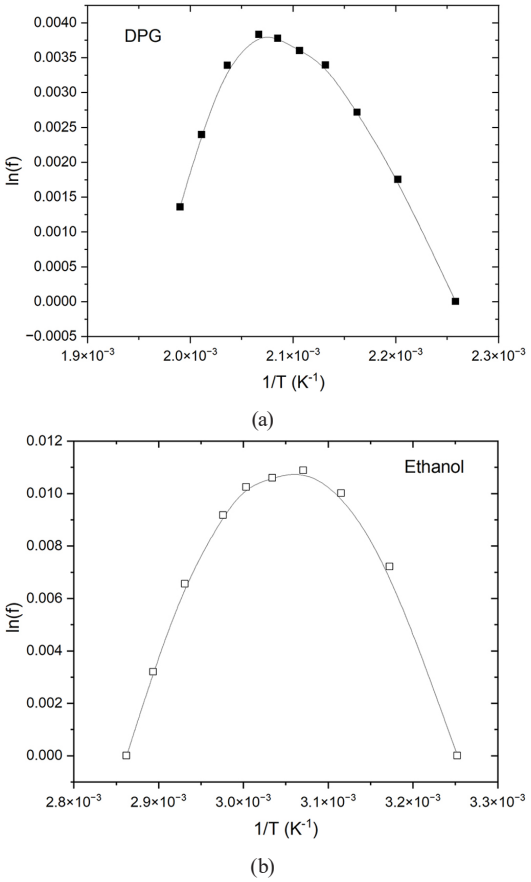

Fig. 3 The results of the arc test applied for the pure components of the binary system Ethanol + DPG: (a) arc test for DPG; (b) arc test for Ethanol.

- γ_i – activity coefficient;
- τ– adjustable parameter;
- α,α' β' – nonrandomness parameters of the NRTL model;
- i, j – i–j interaction pair;
- j, i – j–i interaction pair;
- k – component k.

Eqs. 12–19 are describing the main relations for the UNIQUAC thermodynamic model.

$$ln\gamma_i = ln\gamma_i^{(c)} + ln\gamma_i^{(r)}, \tag{12}$$

$$ln\gamma_i^{(r)} = -q_i ln\left(\sum_j \theta_j \tau_{ji}\right) + q_i - q_i \sum_j \frac{\theta_j \tau_{ij}}{\sum_k \theta_k \tau_{kj}}, \tag{13}$$

$$ln\gamma_i^{(c)} = ln\frac{\varphi_i}{x_i} + \frac{z}{2} q_i ln\frac{\theta_i}{\varphi_i} + l_i - \frac{\varphi_i}{x_i}\sum_j x_j l_j, \tag{14}$$

$$l_j = \frac{z}{2}\left(r_j - q_j\right) - \left(r_j - 1\right), \tag{15}$$

$$\theta_i = \frac{q_i x_i}{\sum_j q_j x_j} \text{ and } \varphi_i = \frac{r_i x_i}{\sum_j r_j x_j}, \tag{16}$$

$$\tau_{ij} = \exp\left(-\frac{U_{ij}}{T}\right), \text{ when unit is K}, \tag{17}$$

$$\tau_{ij} = \exp\left(-\frac{U_{ij}}{RT}\right), \text{ when unit is kcal or kJ}, \tag{18}$$

$$U_{ij} = a_{ij} + b_{ij}T. \tag{19}$$

Where the specific symbols of the UNIQUAC model are:

- l – parameter of the molecule of the UNIQUAC model;
- q – surface area parameter of the UNIQUAC model;
- r – volume parameter of the UNIQUAC model;
- φ – average fraction of the segment in the UNIQUAC model;
- θ – average fraction of the area in the UNIQUAC model;
- z – coordination number of the tridimensional network of the liquid;
- (c) – combinatorial part of the variable;
- (r) – residual part of the variable.

The binary interaction parameters of the NRTL and UNIQUAC models resulting from the regression of experimental data for the ethanol + DPG binary system are presented in Table 3, together with those for water + ethanol found in the PRO/II data bank. Parameters for water + DPG binary system were obtained by regressing the experimental data determined by Fendu and Oprea [33]. The surface area parameter (q) and volume parameter (r) for the components, used in the UNIQUAC thermodynamic model are displayed in Table 4.

Maximum percentage relative deviations resulting from the regression of experimental data for the pressure, temperature, and liquid phase composition of ethanol with the NRTL and UNIQUAC models are shown in Table 5. The maximum percentage deviations for the binary system water + DPG were obtained by regressing the experimental data determined by Fendu and Oprea [33] and using UNIQUAC with four binary interaction parameters as a thermodynamic model.

For the ethanol + DPG binary system, the three variants of the regression using the NRTL model with three, five, and eight parameters show small values of the relative deviations for the pressure. Still, only the NRTL model with eight parameters has an acceptable value for the maximum relative deviation of the liquid phase composition of ethanol. The values of the relative deviations for the pressure resulting from the regression of the experimental using the UNIQUAC model are small for both variants with two and

Table 3 Binary interaction parameters resulted from regression of the experimental data and from the simulation software databank for the systems involved in the study

Binary interaction parameters	Ethanol + DPG NRTL3	Ethanol + DPG NRTL5	Ethanol + DPG NRTL8	Ethanol + DPG UNIQUAC2	Ethanol + DPG UNIQUAC4	Ethanol +water UNIQUAC4*	Water + DPG UNIQUAC4
a_{ij}	-	2.75767	–0.44451	100.97163	–1625.88829	–15.9163	1116.20853
b_{ij}	–218.11509	–1311.37767	–122.50015	-	4.89755	0.239481	–2.97300
c_{ij}	-	-	–12928.87742				
a_{ji}	-	–2.13471	–1.39480	–96.41181	1087.61826	–48.547	–741.89978
b_{ji}	–8.39677	814.59376	104.01110	-	–3.33997	0.344352	1.84396
c_{ji}	-	-	$4.11237 \cdot 10^5$				
α_{ij}	–0.90000	–0.95626	–0.95419				
β_{ij}	-	-	0.00450				

* data from PRO/II data bank [40]

Table 4 Surface area and volume parameter for the components implied in this work, used to calculate the UNIQUAC binary interaction parameters.

Component	Area parameter, q	Volume parameter, r
Ethanol	1.9720	2.1055
DPG	4.6480	5.3503
Water	1.4000	0.9200

Table 5 Maximum percentage relative deviations result from the regression of experimental data with the NRTL and UNIQUAC thermodynamic models

Maximum percentage relative deviation	Ethanol + DPG					Water + DPG
	NRTL 3	NRTL5	NRTL 8	UNIQUAC 2	UNIQUAC 4	UNIQUAC 4
Pressure	1.80	2.07	2.57	1.78	–2.03	1.76
Temperature	$-1.66 \cdot 10^{-3}$	$-1.92 \cdot 10^{-3}$	$-2.44 \cdot 10^{-3}$	$-1.65 \cdot 10^{-3}$	$1.22 \cdot 10^{-3}$	$-2.66 \cdot 10^{-4}$
Concentration of the most volatile component (ethanol or water) in the liquid phase	–22.53	–14.96	8.50	–21.91	9.09	10.79

four parameters. The regression with the UNIQUAC model with four parameters has a lower value of the deviation of the liquid phase composition of ethanol compared to those obtained with UNIQUAC model with two parameters.

For the water + DPG binary system, it can be observed that the values of the relative deviations of pressure and temperature are small, being of the same order of magnitude as for the ethanol + DPG binary system. The maximum relative deviation of the water concentration in the liquid phase is also of the same order of magnitude as the ethanol + DPG binary system.

In Fig. 4 there are displayed the *T-x-y* diagrams for the binary system water + DPG and ethanol + DPG. Fig. 4(a) shows the *T-x-y* diagrams calculated with IDEAL, UNIQUAC, Functional-group Activity Coefficients (UNIFAC) with four parameters, along with the experimental boiling points determined at 28 kPa for the binary system water + DPG. In the simulation software, when UNIFAC predictive model is used to compare the experimental data with the calculated one, DPG is defined using the subgroups displayed in Table 6.

It should be noted that Fig. 4 contain only the experimental data determined at 28 kPa for water + DPG binary system (Fig. 4(a)) and only the experimental data determined at 93.3 kPa for the ethanol + DPG binary system, but in this work were determined VLE data for a broader range of pressure, e.g. 13.3–93.3 kPa.

Table 6 Groups used in the PRO/II simulation software to define the UNIFAC structure of DPG

Associated group number in the simulation program	Number of groups in the structure	Description
200	2	—OH
900	2	—CH_3
901	1	—CH_2—
902	2	—CH— |
601	1	—CH_2—O—

As it can be observed from Fig. 4(a), for the pressure considered (28 kPa), the calculated *T-x* curves have small deviations from experimental data: for small concentrations of water (from 0 up to 0.3 mole fraction water in the

mixture), the UNIQUAC model with four parameters and IDEAL model give similar results, while the bubble point curve calculated with UNIFAC model and experimental data overlaps. Conversely, for higher concentrations of water in the mixture (from 0.5 up to 1 mole fraction water), the experimental data overlap with the bubble points calculated with the UNIQUAC model, while the other two models (UNIFAC and IDEAL) give different results.

The *T-x-y* diagrams calculated with NRTL8, UNIQUAC4, UNIFAC, and IDEAL thermodynamic models and the experimental data determined at 93.3 kPa for the binary system ethanol + DPG are displayed in Fig. 4(b). We can observe in Fig. 4(b) that NRTL8 and IDEAL thermodynamic models give identical results. Instead, the UNIQUAC with four binary interaction parameters and UNIFAC models give similar results but differ from those of IDEAL or NRTL8 models. The experimental boiling points for this mixture, determined at 93.3 kPa, overlap on the bubble points calculated with the UNIQUAC model. These results justify using the UNIQUAC model with four parameters further in the modeling and simulating the water + ethanol separation process by extractive distillation with DPG as an extractive agent.

The relative deviations of calculated temperature with thermodynamic models IDEAL, UNIFAC, NRTL and UNIQUAC, versus experimental temperature were represented in Fig. 5 where from it can be observed that for both binaries, the lowest relative deviations of the calculated bubble points from the experimental bubble points are those corresponding to UNIQUAC model.

The simulation of any process requires adequate and complete thermodynamic models, which is why the equilibrium data for the ethanol + DPG binary system were determined. The equilibrium data we found, together with those existing in the data bank for the ethanol + water binary, constitute a complete thermodynamic model for the simulation of the ethanol anhydrization process by extractive distillation with DPG.

In the simulations of the process presented in this work, we decided to use the UNIQUAC model with four parameters because it has the smallest value of the maximum percentage relative deviation for the pressure. Also, the value of the deviation of the liquid phase composition is close to the minimum resulting in all the regression variants. Also, we must specify that the simulation of the process using NRTL as thermodynamic model was also tried, but the convergence of the EDC column wasn't achieved, a problem that was not encountered when UNIQUAC4 was used for the

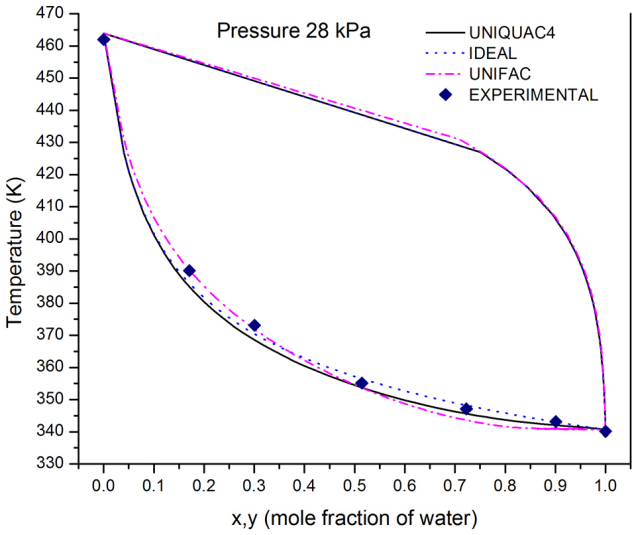

(a)

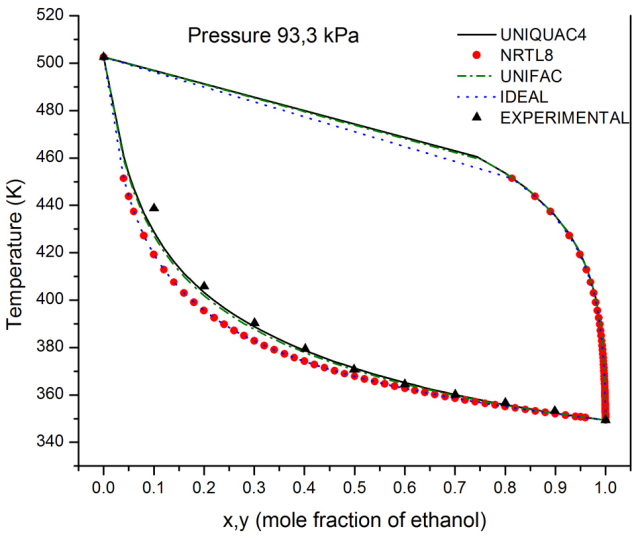

(b)

Fig. 4 *T-x-y* diagrams calculated with different thermodynamic models for the binary systems: (a) water + DPG; (b) ethanol + DPG

simulations. For these reasons, we decided to use for further simulations the UNIQUAC thermodynamic model.

3 Calculation and simulation of the process

3.1 Process description

According to international standards (EN 15376, ASTM D 4806)[3], the bioethanol used as an additive in blend with gasoline must have a minimum purity of 97.48 mole%. The bioethanol obtained from biomass is a diluted solution of ethanol (2.02–4.16 mole% ethanol in water) that must be separated from water and processed (dried) before being added to gasoline. The separation of ethanol from water consists mainly of two steps respectively: a concentration step, where the concentration of

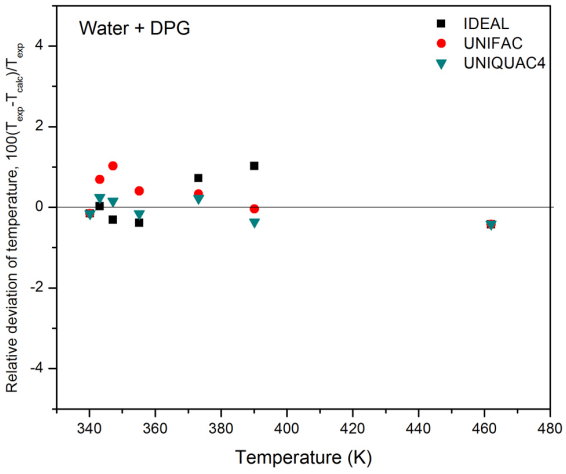

(a)

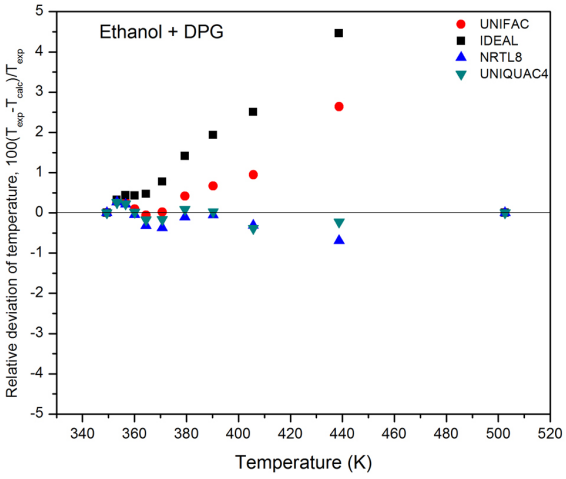

(b)

Fig. 5 Relative deviations of the bubble point temperatures calculated with different thermodynamic models for the two binaries implied in this work: a) relative deviations of bubble points calculated at 28 kPa for the binary water+DPG; b) relative deviations of bubble points calculated at 93.3 kPa for the binary ethanol+DPG.

ethanol in water is raised to 85 mole %, and an advanced drying step, where ethanol is obtained with a purity over 99.49 mole% overcoming the composition of the azeotrope water + ethanol of 89.5 mole% ethanol at atmospheric pressure. The separation of ethanol in the region with an ethanol concentration greater than the azeotrope's concentration is possible due to the dipropylene glycol solvent's influence on the relative volatility of the ethanol + water mixture.

The influence of the DPG on the non-ideality of the mixture of ethanol + water can be observed in Fig. 6, where the equilibrium diagrams *y-x* at atmospheric pressure are plotted for different molar solvent/feed ratios. The ethanol concentration values are calculated considering

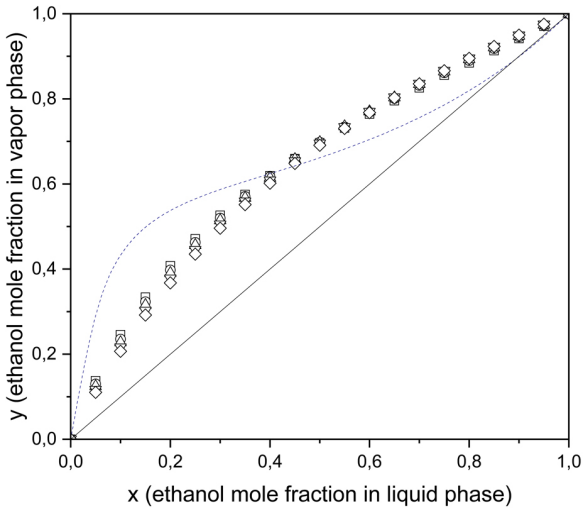

Fig. 6 Influence of DPG solvent on the relative volatility of ethanol (1) + water (2) mixture at atmospheric pressure for the different solvent to feed molar ratio (S/F): dash line – S/F=0; square – S/F=0.2; circle – S/F=0.3; up triangle – S/F=0.4; down triangle – S/F=0.6; diamond – S F=0.8.

the presence of the DPG in the mixture. The *y-x* diagrams were generated using PRO /II simulation software.

It can be observed that the presence of DPG broke the azeotrope ethanol + water, all curves for different molar solvent/feed ratios (from 0.2 to 0.8), indicating a quasi-ideal mixture. Withal, it can be observed that the differences in relative volatilities are not significant from one ratio to another (positions of the *y-x* curves do not vary too much). Considering this, we can assume to work at a small molar solvent/feed ratio (0.3–0.4) because a high solvent/feed ratio means a large amount of solvent used to achieve the same desired ethanol purity and, ultimately, high energy consumption for the solvent recovery column. But the final decision will be highlighted by the sensitivity analysis regarding the effect of the solvent/feed ratio on the total reboiler duty and implicitly on the specific energy consumption of the process.

In this work, the feasibility of DPG as an extractive agent is studied in a classic extractive distillation installation and an improved variant with thermal integration. The process simulation diagrams are shown in Figs. 7, 8. The concentration step is realized in an ordinary distillation column, the pre-concentration column (PC). Here, the ethanol concentration in the feed stream is increased from 4.16 mole% up to 82.7 mole% in the distillate. A stream of 99.98 mole% of water is obtained at the bottom of the PC column. The drying step (anhydrization) is realized by extractive distillation with DPG in the extractive

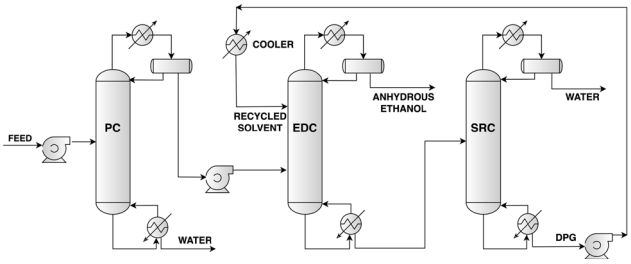

Fig. 7 Process flowsheet diagram of ethanol anhydrization by extractive distillation with dipropylene glycol – variant A.

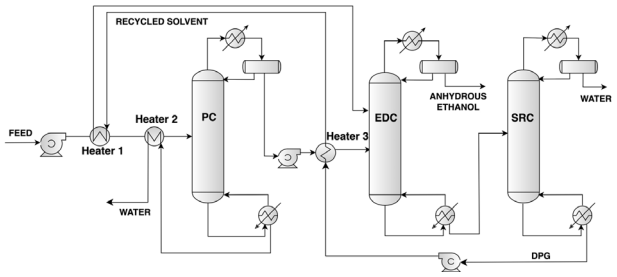

Fig. 8 Process flowsheet diagram of ethanol anhydrization by extractive distillation with dipropylene glycol – variant B

distillation column (EDC); the ethanol obtained as distillate has a purity over 99.74 mole% (corresponding to 99.9 mass%) –the minimum necessary to be used as an additive in the gasoline. The regeneration of the solvent is realized in the solvent regeneration column (SRC). The DPG obtained as the bottom product from SRC has a purity of 99.93 mole%. Two base case simulation variants were studied, using in simulations different solvent to feed molar ratios (S/F), from 0.385 to 0.731 kmol DPG/kmol ethanol + water mixture, all being realized in PRO II 2020 (from AVEVA) [42] and using the UNIQUAC thermodynamic model, completed with the binary interaction parameters determined in Section 2. The simulation's first base case (variant A – see Fig. 7) is the conventional installation, with three columns and no heat recovery.

The second base case – variant B (see Fig. 8) is considering the heat recovery from the regenerated solvent hot stream. In both simulation variants, the distillation columns operate at atmospheric pressure. To reduce the reboiler duties to the PC and EDC column, two heat exchangers, Heater 1 and Heater 2, are provided on the feed stream of the PC column, and heat exchanger Heater 3 heats the stream that feeds the extractive distillation column. The heat exchangers Heater 3 and Heater 1 recover the heat from the hot stream of regenerated solvent. The hot regenerated solvent coming from the bottom of the SRC column first preheats the feeding stream of the EDC column in Heater 3, and the remaining heat is used further to preheat the feeding stream of the PC column in Heater 1. Then, the cooled regenerated solvent is returned to the top of the EDC column. The heat exchanger Heater 2 cools the water separated in the bottom of the PC column and, meanwhile, heats the feeding stream of the PC column (previously pre-heated in Heater 1) to the temperature corresponding to the feeding tray temperature.

3.2 Results and discussions for the process simulation

Both variants A and B, were simulated in the same working conditions: the feed flowrate and composition of the feeding stream, the number of trays in the three distillation columns, the feeding tray for each column, and the purity and recoveries of the products are identical. The number of the theoretical trays in the columns has been chosen considering the previous works in the literature [4, 6, 7], adjusting the number of trays and the feeding tray as necessary to obtain the desired results: a stream of pure water in the bottoms of the PC column (99.98 mole% water), a high purity anhydrous ethanol (99.74 mole%), and a high purity regenerated solvent (over 99.9 mole% DPG), all these with good recoveries, over 99.9%. Many simulations were made until the best operation parameters were established. A shortcut distillation model was used for the preconcentration column, and the number of trays resulted was multiplied by two and then used in the rigorous simulation. The shortcut method cannot be applied for the EDC column, which separates a strong non-ideal system. The number of trays was chosen first as in the similar processes described in the literature [7, 32] and then increased until the best variant was found. For this aim, the concentration of water and ethanol in the distillate product was followed depending on the number of theoretical trays, number of the feed stage, reflux ratio, and solvent to feed ratio. Also, the distillate flowrate and the DPG concentration in the anhydrous ethanol were followed for the extractive distillation column, depending on the number of theoretical trays. A shortcut distillation model was used for the solvent regeneration column, and the resulting number of trays was used in the rigorous simulation. In Table 7 are given the operating conditions mentioned previously for both variants A and B.

As it was mentioned before, both base cases, A and B, were simulated using different solvent /feed (EDC column feed) molar ratio, respectively, we used the following S/F values: 0.385, 0.455, 0.525, 0.595, 0.665, 0.731 kmol DPG/kmol (ethanol + water) mixture. Obviously, the ethanol + water mixture refers to the feeding stream of the EDC column and has the same composition as the distillate product of the PC

Table 7 Design parameters of the ethanol anhydrization process by extractive distillation with DPG for base case A and B

Design parameters		Pre-concentration *n* column (PC)	Extractive distillation column (EDC)	Solvent recovery column (SRC)
Top tray pressure, kPa		101	101	100
Bottom tray pressure, kPa		129	136	104
Number of trays		30	37	16
Reflux molar ratio		3	1.83 (variant A) 1.98 (variant B)	1.15
Feed tray		19	25	7
Feed tray of extractive agent		-	6	-
Feed flowrate (kmole/h)		849.5	42.36	27.95
Feed composition (mole%)	ethanol	4.16	82.95	0.013
	water	95.84	17.05	25.33
	DPG	0	0	74.66

column. The results of the sensitivity analysis regarding the effect of S/F ratio on the specific energy consumption (SEC) for variants A and B are displayed in Fig. 9.

As it can be observed in Fig. 9, the specific energy consumption (SEC) calculated as total reboiler duty (the sum of the reboiler duties for all three distillation columns) over the flowrate of anhydrous ethanol (1624.11 kg ethanol /h) decreases with the increase of the S/F, and at first glance,

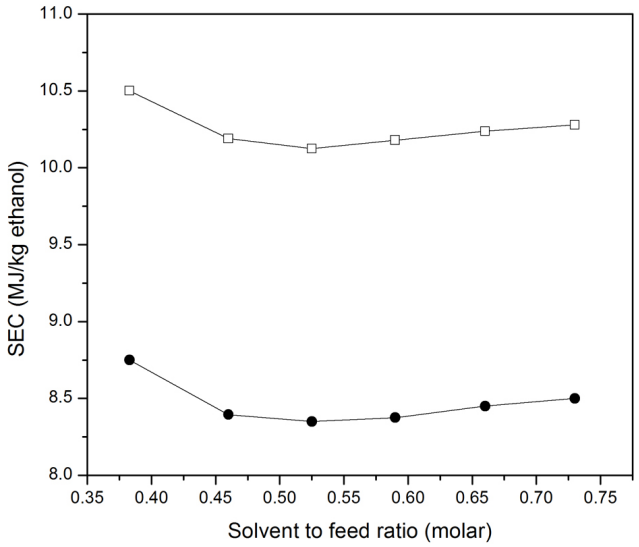

Fig. 9 The solvent (DPG) flowrate influence on the specific energy consumption: open square - specific energy consumption for variant A; full circle– specific energy consumption for variant B.

this can appear contradictory. This fact can be explained by the reflux ratio of the extractive distillation column: when solvent flowrate increases, a small reflux ratio is necessary to obtain the desired purity of the ethanol, and as a consequence, a smaller quantity of liquid is circulated in the column; on the other hand, when a reduced flowrate of solvent DPG is used, a high reflux ratio is necessary to attain the high purity of ethanol, this meaning a high quantity of liquid in the column and in the reboiler to be heated.

Following the variation of SEC with the S/F ratio, it can be observed that the variation curves for both base case A and B exhibit a minimum value corresponding to a solvent/feed molar ratio of 0.491. There were performed simulations for both base cases, using the value of S/F = 0.491. The results of these best operation variants of cases A and B (named subsequently variant A(best) and variant B (best)) are displayed in Table 8, Fig. 10, and Fig. 11.

As it is shown in Table 8, in both simulation variants, A(best) and B (best), the component of interest, ethanol, is recovered in the EDC column as anhydrous ethanol with a purity of 99.8 mole% (corresponding to 770 mass ppm of water), greater than the minimum imposed to be used with gasoline. The significant quantity of water entered in the installation with the ethanol is removed in the PC column, where 99.11 % of the water is obtained in this column as the bottom product.

The remaining water is removed in the EDC column, being "solubilized" by the extractive agent – DPG. In the EDC column, anhydrous ethanol (99.8 mole%) is obtained at the top of the column with a high recovery grade of 99.99%. The extractive agent – DPG, is regenerated in the SRC column; here, the water solubilized by DPG is recovered in a proportion of 99.45% as distillate, while in the bottom of the column is recovered the extractive agent with a purity of 99.93 mole%.

Variant B is an improved simulation variant that considers heat recovery from the PFD's hot streams. Two heat exchangers are considered on the hot stream of regenerated solvent, Heater 3 and Heater 1. The hot regenerated solvent coming from the bottom of the SRC column (stream 14) with 505.65 K first preheats the feeding stream of the EDC column (stream 8) in Heater 3 from 351.29 K to 356.89 K. Thus, the regenerated solvent cools up to 366.15 K (stream 15). In Heater 1, the regenerated solvent cools further, from 366.15 K to 352.15 K (the temperature on the feeding tray with solvent in the EDC column), and preheat the feeding stream of the PC column, from 313.15 K (stream 2) to 314.78 K (stream 3). The heat exchanger Heater 2 cools the water separated in the bottom of the PC column (stream 6) from 380.06 K up to

Table 8 Simulation results for best variants A and B, with a S/F ratio of 0.491 kmole DPG/ kmole feed ethanol + water mixture

Design parameters	Pre-concentration column (PC)	Extractive distillation column (EDC)	Solvent recovery column (SRC)
Feed flowrate, kmole/h	849.5	42.36	27.95
Pressure of the feed stream, kPa	106	126	136
Feed composition (mole%)			
ethanol	4.16	82.95	0.013
water	95.84	17.05	25.33
DPG	0	0	74.66
Feed flowrate of extractive agent (kmole/h)			
Variant A	-	20.87	-
Variant B	-	20.87	-
Top pressure, kPa			
Variant A	101	101	100
Variant B	101	101	100
Column pressure drop, kPa (both variants)	29	39	4
Reboiler duty, MJ/h			
Variant A	10917	4517	1282
Variant B	7404	3523	1292
Condenser duty, MJ/h			
Variant A	6640	3861	622
Variant B	6659	4070	629
Distillate flowrate, kmole/h	42.36	35.3	7.07
Composition of the distillate product (mole%)			
ethanol	82.95	99.8	0.05
water	17.05	0.2	99.92
DPG	0	0	0.03
Bottom product flowrate, kmole/h	807.14	27.95	20.88
Composition of the bottom product (mole%)			
ethanol	0.02	0.013	0
water	99.98	25.33	0.07
DPG	0	74.66	99.93
Ethanol recovery, %	99.55	99.99	-
Water recovery, %	99.11	99.26	99.49
Dipropylene glycol recovery, %	-	100	100

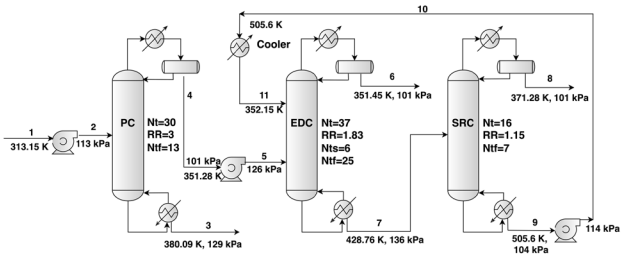

Fig. 10 Process simulation diagram of ethanol anhydrization by extractive distillation with dipropylene glycol for the variant A (best): Ntt-number of theoretical trays; RR- reflux ratio (molar); Ntf-number of feeding tray; Nts- number of feeding tray with solvent.

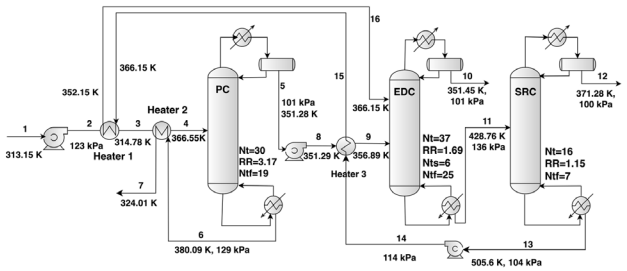

Fig. 11 Process simulation diagram of ethanol anhydrization by extractive distillation with dipropylene glycol for variant B (best): Ntt-number of theoretical trays; RR- reflux ratio (molar); Ntf-number of feeding tray; Nts- number of feeding tray with solvent.

324.01 K and meanwhile heats the feeding stream of the PC column, previously pre-heated in Heater 1 (stream 3) from 314.78 K up to 366.55 K – the temperature corresponding to the feeding tray temperature.

The temperature and flowrate profiles of the columns for both best variants can be found in Figs. S6–S11 of the Supplement. Also, in the Supplement, the variation of the composition of vapor and liquid phases can be found for all columns and both simulation variants in Figs. S12–S17.

Considering the reboiler duties displayed in Table 8 for best variants A and B and the flowrate of the anhydrous ethanol obtained, we calculated for variant A the SEC of 10.29 MJ/kg anhydrous ethanol, while for variant B the SEC is lower, being equal to 7.53 MJ/kg of anhydrous ethanol. The specific energy consumptions obtained in this work are comparable with those obtained by other researchers for similar processes, as shown in Table 9.

The specific energy consumption obtained using the solvent ethylene glycol or isooctane is lower than the SEC calculated in the current work for variant A, where no heat recovery was considered. This fact is due to EG and isooctane's lower boiling point than DPG. These two solvents are more volatile than dipropylene glycol. Also, it can be observed in Table 9 that there are differences between the

Table 9 Specific energy consumptions for different processes of ethanol anhydrization by extractive distillation

Type of the process	Extractive agent	Ethanol in the initial solution (wt.%)	SEC (MJ/kg ethanol)
Extractive distillation	DPG (this study)	10	10.29 (without heat recovery) 7.53 (with heat recovery)
Extractive distillation	EG	10	8.05 [4]
Extractive distillation	Isooctanol	12	11.42 [5]
Extractive distillation	Isooctane	10	8 [15]
Extractive distillation	EG	10	8.892 [8]
Liquid-liquid extraction combined with extractive distillation	Octanoic acid	12	13.35 [5]

results of the processes using the same solvent (i.e., EG). These differences appear because of the arrangement and configuration of the columns and due to the integrated heat configurations. On the other hand, the SEC obtained for the processes using less volatile solvents (such as octanoic acid) is higher due to the solvent's higher boiling points. Nevertheless, variant B proposed in this work is the most convenient considering energy consumption.

The results of the simulations presented in this paper demonstrate the ability of DPG as an extractive agent in the separation of the ethanol + water mixture. Along with the simulations with the completed UNIQUAC model, simulations of the process using the UNIFAC predictive model were also performed. Thus, it could be found that when the UNIFAC model was employed as the thermodynamic model for process simulation, a molar flow rate of DPG solvent was required that was more than twice that we used in the simulations where UNIQUAC 4 was employed as a thermodynamic model. This finding further reinforces the idea of the need to use experimental data in process calculations, as is done in this paper, and use predictive models such as UNIFAC only for preliminary calculations.

4 Conclusions

This study presents experimental vapor-liquid equilibrium data between ethanol and dipropylene glycol and the results of two variants of simulation of the anhydrization process of ethanol by extractive distillation using as solvent dipropylene glycol. The VLE data were determined as *P-T-x* data (temperature boiling points at constant pressure) with an equilibrium apparatus built in our laboratory. The vapor-liquid equilibrium data were regressed in PRO/II 2020, and binary parameters of two models, NRTL and UNIQUAC, were obtained. The set of binary parameters corresponding to the slightest deviation for pressure, temperature, and composition in the liquid phase of ethanol (UNIQUAC 4) was used in the water + ethanol separation simulation by extractive distillation with DPG. The equilibrium data determined in this study for the ethanol + DPG binary, together with the data for water + DPG binary and those existing in the data bank of the simulation software for the ethanol + water binary, constitute a complete thermodynamic model for the adequate simulation of the ethanol anhydrization process by extractive distillation with DPG.

For the study of water + ethanol separation process by extractive distillation with DPG, were realized a series of several simulations, starting from two base cases: a base case where no heat recovery is considered (variant A) and a base case where the heat of two hot streams from the process is recovered as much as possible (variant B). All the simulations were realized using similar operating conditions (number of trays in the columns, feed flowrate, solvent flowrate, specification of final products). Using the results from all the simulations, a sensitivity analysis was realized regarding the effect of the S/F ratio on the specific energy consumption. It was found that for a solvent/feed molar ratio of 0.491, the SEC exhibits a minimum for both variants A and B. Thus, it was found that for variant A, considering a S/F = 0.491 kmol DPG/ kmole (ethanol + water) mixture, the SEC is 10.29 MJ/kg of anhydrous ethanol, while in variant B, for the same S/F, the SEC is 7.53 MJ/kg of anhydrous ethanol. The specific energy consumption values obtained for the variants simulated in this work are comparable with the specific energy consumptions obtained by other researchers with similar extractive distillation processes using different solvents. Variant B proposed in this work has the lowest SEC compared with other extractive agents reported by other researchers and is the most convenient if we consider energy consumption. Also, it must be taken into account that DPG, even if it is a superior glycol with an increased boiling point compared to other glycols (1.3PG, DEG, EG), has excellent solvency properties, and it can be used in smaller ratios (as in this study, the S/F was 0.491). Implicitly the solvent consumption is lower compared to other extractive distillation processes. Moreover, the extractive distillation process for the anhydrization of ethanol with DPG can be used in the existing installations with no considerable capital costs.

References

[1] European Committee for Standardization "EN 228:2012+A12017 automotive fuels. Unleaded petrol-requirements and test methods", European Committee for Standardization Brusseles, Belgium, 2017.

[2] Balat, M. "Production of bioethanol from lignocellulosic materials via the biochemical pathway: a review", Energy Conversion and Management, 52(2), pp. 858–875, 2011. https://doi.org/10.1016/j.enconman.2010.08.013

[3] European Committee for Standardization "EN 15376/2014 – Automotive fuels – ethanol as a blending component for petrol – requirements and test methods", European Committee for Standardization, Brusseles, Belgium, 2017.

[4] Pătrașcu, I., Bîldea, C. S. "Controllability of bioethanol dehydration process using a pressure-driven dynamic model", Bulletin of Romanian Chemical Engineering Society, 2, pp. 19–27, 2015. [online] Available at: http://sicr.ro/wp-content/uploads/2015/07/BRChES_vol.2_nr.1_2015.pdf#page=21 [Accessed: 30 January 2024]

[5] Vázquez-Ojeda, M., Segovia-Hernández, J. G., Hernández, S., Hernández-Aguirre, A., Kiss, A. A. "Design and optimization of an ethanol dehydration process using stochastic methods", Separation and Purification Technology, 105, pp. 90–97, 2013. https://doi.org/10.1016/j.seppur.2012.12.002

[6] Kiss, A. A., Suszwalak, D. J.-P. C. "Efficient bioethanol dehydration in azeotropic and extractive dividing-wall columns", Procedia Engineering, 42, pp. 566–572, 2012. https://doi.org/10.1016/j.proeng.2012.07.449

[7] Kiss, A. A., Suszwalak, D. J.-P. C. "Enhanced bioethanol dehydration by extractive and azeotropic distillation in dividing-wall columns", Separation and Purification Technology, 86, pp. 70–78, 2012. https://doi.org/10.1016/j.seppur.2011.10.022

[8] Kiss, A. A., Ignat, R. M. "Innovative single step bioethanol dehydration in an extractive dividing-wall column", Separation and Purification Technology, 98, pp. 290–297, 2012. https://doi.org/10.1016/j.seppur.2012.06.029

[9] Gil, I. D., Gómez, J. M., Rodríguez, G. "Control of an extractive distillation process to dehydrate ethanol using glycerol as entrainer", Computers and Chemical Engineering, 39, pp. 129–142, 2012. https://doi.org/10.1016/j.compchemeng.2012.01.006

[10] Soares, R. B., Pessoa, F. L. P.,Mendes, M. F. "Dehydration of ethanol with different salts in a packed distillation column", Process Safety and Environmental Protection, 93, pp. 147–153, 2015. https://doi.org/10.1016/j.psep.2014.02.012

[11] Pan, Q., Shang, X., Li, J., Ma, S., Li, L., Sun, L. "Energy-efficient separation process and control scheme for extractive distillation of ethanol-water using deep eutectic solvent", Separation and Purification Technology, 219, pp. 113–126, 2019. https://doi.org/10.1016/j.seppur.2019.03.022

[12] Shang X., Ma, S., Pan, Q., Li, J., Sun, Y., Ji, K., Sun, L. "Process analysis of extractive distillation for the separation of ethanol–water using deep eutectic solvent as entrainer", Chemical Engineering Research and Design, 148, pp. 298–311, 2019. https://doi.org/10.1016/j.cherd.2019.06.014

[13] Ma, S., Hou, Y., Sun,Y., Li, J., Li, Y., Sun, L. "Simulation and experiment for ethanol dehydration using low transition temperature mixtures (LTTMs) as entrainers", Chemical Engineering and Processing: Process Intensification, 121, pp. 71–80, 2017. https://doi.org/10.1016/j.cep.2017.08.009

[14] Pleșu Popescu, A. E., Pellin, J. L., Bonet, J., Llorens, J. "Bioethanol dehydration and mixing by heterogeneous azeotropic distillation", Journal of Cleaner Production, 320, 128810, 2021. https://doi.org/10.1016/j.jclepro.2021.128810

[15] Li, J., You, C., Lyu, Z., Zhang, C., Chen, L., Qi, Z. "Fuel-based ethanol dehydration process directly extracted by gasoline additive", Separation and Purification Technology, 149, pp. 9–15, 2015. https://doi.org/10.1016/j.seppur.2015.05.012

[16] Pleșu Popescu, A. E., Pellin, J. L., Bonet-Ruiz, J., Llorens, J. "Cleaner process and entrainer screening for bioethanol dehydration by heterogeneous azeotropic distillation", Chemical Engineering Transactions, 81, pp. 829–834, 2020. https://doi.org/10.3303/CET2081139

[17] Gomis, V., Pedraza, R., Saquete, M. D., Font, A. García-Cano, J. "Ethanol dehydration via azeotropic distillation with gasoline fraction mixtures as entrainers: a pilot-scale study with industrially produced bioethanol and naphta", Fuel Processing Technology, 140, pp. 198–204, 2015. https://doi.org/10.1016/j.fuproc.2015.09.006

[18] Chianese, A. Zinnamosca, F. "Ethanol dehydration by azeotropic distillation with a mixed-solvent entrainer", The Chemical Engineering Journal, 43(2), pp. 59–65, 1990. https://doi.org/10.1016/0300-9467(90)80001-S

[19] Khalid, A., Aslam, M., Qyyum, M. A., Faisal, A., Khan, A. L., Ahmed, F., Lee, M., Kim, J., Jang, N., Chang, I. S., Bazmi, A. A., Yasin, M. "Membrane separation processes for dehydration of bioethanol from fermentation broths: recent developments, challenges, and prospects", Renewable and Sustainable Energy Reviews, 105, pp. 427–443, 2019. https://doi.org/10.1016/j.rser.2019.02.002

[20] Wang, Y., Gong, C., Sun, J., Gao, H., Zheng, S., Xu, S. "Separation of ethanol/water azeotrope using compound starch-based adsorbents", Bioresource Technology, 101(15), pp. 6170–6176, 2010. https://doi.org/10.1016/j.biortech.2010.02.102

[21] Roth, T., Kreis, P., Górak, A. "Process analysis and optimisation of hybrid processes for the dehydration of ethanol", Chemical Engineering Research and Design, 91(7), pp. 1171–1185, 2013. https://doi.org/10.1016/j.cherd.2013.01.016

[22] Hanchate, N., Kulshreshtha, P., Mathpati, C. S. "Optimization, scale-up and cost estimation of dehydration of ethanol using temperature swing adsorption", Journal of Environmental Chemical Engineering, 7(2), 102938, 2019. https://doi.org/10.1016/j.jece.2019.102938

[23] Leppäjärvi, T., Malinen, I., Korelskiy, D., Kangas, Hedlund, J., Tanskanen, J., "Pervaporation of ethanol/water mixtures through a high-silica MFI membrane: comparison of different semi-empirical mass transfer models", Periodica Polytechnica Chemical Engineering, 59(2), pp. 111–123, 2015. https://doi.org/10.3311/PPch.7665

[24] Valentínyi, N., Mizsey, P. "Comparison of pervaporation models with simulation of hybrid separation processes", Periodica Polytechnica Chemical Engineering, 58(1), pp. 7–14, 2014. https://doi.org/10.3311/PPch.7120

[25] Singh, A., Cunha, S., Rangaiah, G. P., "Heat-pump assisted distillation versus double-effect distillation for bioethanol recovery followed by pressure swing adsorption for bioethanol dehydration", Separation and Purification Technology, 210, pp. 574–586, 2019. https://doi.org/10.1016/j.seppur.2018.08.043

[26] Loy, Y. Y., Lee, X. L., Rangaiah, G. P. "Bioethanol recovery and purification using extractive dividing-wall column and pressure swing adsorption: an economic comparison after heat integration and optimization", Separation and Purification Technology, 149, pp. 413–427, 2015. https://doi.org/10.1016/j.seppur.2015.06.007

[27] Botshekan, M., Moheb, A., Vatankhah, F., Karimi, K., Shafiei, M. "Energy saving alternatives for renewable ethanol production with the focus on separation/purification units: a techno-economic analysis", Energy, 239, 122363, 2022. https://doi.org/10.1016/j.energy.2021.122363

[28] Tututi-Avila, S., Jiménez-Gutiérrez, A., Hahn, J. "Control analysis of an extractive dividing-wall column used for ethanol dehydration", Chemical Engineering and Processing: Process Intensification, 82, pp. 88–100, 2014. https://doi.org/10.1016/j.cep.2014.05.005

[29] The Dow Chemical Company "Safety data sheet Product name: dipropylene glycol regular grade", The Dow Chemical Company, 2023. [online] Available at: https://www.dow.com/en-us/doc-viewer-blank.html?docType=SDS&contentType=SDS&product=21603z&tradeProduct=000000021603&selectedCountry=US&selectedLanguage=EN&recordNumber=49205848&title=Dipropylene%20Glycol%20(DPG)%20Regular%20Grade-Safety%20Data%20Sheet-EN&useRequestPath=true [Accessed: 15 January 2024]

[30] Nicolae, M., Oprea, F., Fendu, E. M. "Dipropylene glycol as a solvent for the extraction of aromatic hydrocarbons. Analysis and evaluation of the solvency properties and simulation of the extraction processes", Chemical Engineering Research and Design, 104, pp. 287–295, 2015. https://doi.org/10.1016/j.cherd.2015.08.021

[31] Nicolae, M., Oprea, F. "Vapor–liquid equilibrium for the binary mixtures of dipropylene glycol with aromatic hydrocarbons: Experimental and regression", Fluid Phase Equilibria, 370, pp. 34–42, 2014. https://doi.org/10.1016/j.fluid.2014.03.003

[32] Neagu M., Cursaru, D. L. "Bioethanol dehydration by extractive distillation with propylene glycol entrainer", Revista de Chimie, 64(1), pp. 92–94, 2013.

[33] Fendu, E. M., Oprea, F., "Vapor–liquid equilibria for water + propylene glycols binary systems: experimental data and regression", Journal of Chemical and Engineering Data, 59(3), pp. 792–801, 2014. https://doi.org/10.1021/je4009014

[34] Fredenslund, A., Jones, R. L., Prausnitz, J. M. "Group-contribution estimation of activity coefficients in nonideal liquid mixtures" AIChE Journal, 21, pp. 1086–1099, 1975. https://doi.org/10.1002/aic.690210607

[35] Prausnitz, J. M., Lichtenthaler, R. N., Azevedo, E. G. "Molecular thermodynamics of fluid-phase equilibria" 3rd ed., Prentice Hall PTR: NJ, 1999.

[36] Van Der Linde, P. R., Blok, J. G., Oonk, H. A. J. "Naphthalene as a reference substance for vapour pressure measurements looked upon from an unconventional point of view", The Journal of Chemical Thermodynamics, 30(7), pp. 909–917, 1998. https://doi.org/10.1006/jcht.1998.0357

[37] Oonk, H. A. J., Van Der Linde, P. R. Huinink, J., Blok, J. G. "Representation and assessment of vapour pressure data; a novel approach applied to crystalline 1-bromo-4-chlorobenzene, 1-chloro-4-iodobenzene, and 1-bromo-4-iodobenzene", The Journal of Chemical Thermodynamics, 30(7), pp. 897–907, 1998. https://doi.org/10.1006/jcht.1998.0356

[38] National Institute of Standard and Technology "VLE thermodynamic consistency: pure component consistency test background", [online] Available at: https://trc.nist.gov/TDE/Help/TDE103b_v4_0/VLE-DataSets-ConsistencyTests/Pure.htm [Accessed: 07 January 2024]

[39] Kang, J. W., Diky, V., Chirico, R. D., Magee, J. W., Muzny, C. D., Abdulagatov, I., Kazakov, A. F., Frenkel, M. "Quality assessment algorithm for vapor−liquid equilibrium data", Journal of Chemical and Engineering Data, 55(9), pp. 3631–3640, 2010. https://doi.org/10.1021/je1002169

[40] Renon, H., Prausnitz, J. M. "Local compositions in thermodynamic excess functions for liquid mixtures", AIChE Journal, 14(1), pp. 135–144, 1968. https://doi.org/10.1002/aic.690140124

[41] Abrams, D. S., Prausnitz, J. M. "Statistical thermodynamics of liquid mixtures: a new expression for the excess Gibbs energy of partly or completely miscible systems", AIChE Journal, 21(1), pp. 116–128, 1975. https://doi.org/10.1002/aic.690210115

[42] Aveva "PRO/II Aveva software, (2020)", Aveva LLC, South Lake Forest, CA, 2022. [computer program] Available at: https://www.aveva.com/en/products/pro-ii-simulation/